# Intercomparison between two approaches for improving the resolution of Doppler-velocity coherent-lidar profiles

Tanja N. Dreischuh, Ljuan L. Gurdev, and Dimitar V. Stoyanov

Institute of Electronics, Bulgarian Academy of Sciences
72 Tzarigradsko Chaussee, 1784 Sofia, Bulgaria

## ABSTRACT

The feasibilities of a new approach for improving the resolution of coherent Doppler lidars, compared with the known PP-estimator-based approach, are investigated by computer simulations in the case of rectangular laser pulses. This approach consists in employing inverse techniques for retrieving the Doppler-velocity profile on the basis of known pulse shape and estimated statistically autocovariance of the heterodyne-signal profile. The possibility is demonstrated to achieve a spatial resolution cell that is much shorter than the pulse length.

**Keywords:** coherent Doppler lidar, pulsed lidar, lidar resolution

## 1. INTRODUCTION

A natural approach for improving the resolution of coherent Doppler lidars is to use as short as possible sensing laser pulses. Thereat, the pulse duration should be at least an order of magnitude longer than the oscillation period of the heterodyne signal in order to estimate accurately the Doppler velocity profiles. Except the pulse duration (length), another factor determining the spatial resolution is the interval of averaging along the line of sight, as is for instance in the case of employing pulse-pair (PP) or poly-pulse-pair (PPP) algorithms[1] for estimation of Doppler velocity. Recently we have developed[2] another approach for improving the resolution of coherent Doppler lidars. This approach consists in employing inverse techniques for retrieving the Doppler-velocity profile on the basis of known pulse shape and estimated statistically autocovariance of the heterodyne-signal profile. It allows one to achieve in principle a spatial resolution cell that is much shorter than the pulse length, but at the expense of an increase of the speckle-noise effect that leads to lowering the temporal resolution.

The purpose of the present work is to investigate by computer simulations the advantages and limitations of the latter approach, compared with the PP-estimator-based approach, in the case of rectangular laser pulses as well as to search for ways to essentially reduce the speckle-noise effect and thus increase the temporal resolution.

## 2. COHERENT LIDAR RETURN SIGNAL

We shall consider the coherent lidar return signal as a complex photocurrent $I(t)=J(t)+jQ(t)$ resulting from quadrature heterodyne detection of pulsed laser source radiation incoherently backscattered by atmospheric aerosol particles; $J(t)$ is inphase component, $Q(t)$ is quadrature component, $t$ is the time interval after the pulse emission, and $j$ is imaginary unity. In the case of rectangular laser pulses the pulse shape $f(\theta)=1$ for $\theta\in[0,\tau]$, and $f(\theta)=0$ elsewhere; $f(\theta)=P(\theta)/P_p$, $P(\theta)$ is the pulse power profile with peak value $P_p$, $\theta$ is a time variable, and $\tau$ is the pulse duration. Then the expression of $I(t)$ has the form[2-5]:

$$I(t=2z/c)=\int_{\varphi(t)}^{ct/2} dz'[\Phi(z')]^{1/2} w(z')\exp[j\omega_m(z')t] \quad , \tag{1}$$

where $z=ct/2$ is the pulse front position; $\varphi(t)=z_o$ when $z-z_o\le c\tau/2$ and $\varphi(t)=c(t-\tau)/2$ when $z-z_o\ge c\tau/2$; $z_o=ct_o/2$ is the coordinate along the line of sight (Oz) of the initial scattering volume contributing to the signal; $c$ is the speed of light; $\Phi(z)$ is the maximum-resolved lidar power profile[6]; $\langle w^*(z)w(z+\Delta z)\rangle=\delta(\Delta z)$; $\langle.\rangle$, $\delta$, and „*“ denote ensemble average, delta function, and complex conjugation respectively; $\omega_m(z)=\omega_o[1-V(z)/c]-\omega_h$ is intermediate frequency, $\omega_o$ is the sensing radiation frequency, $\omega_h$ is the local oscillator frequency, and $V(z)$ is the radial aerosol velocity distribution. Here we do not consider the effects of frequency chirp and radial-velocity fluctuations. The discrete analog of Eq.(1) is:

$$I(t_{l_2}=2z_{l_2}/c)=\sum_{l=b}^{l_2}[\Phi(z_l)\Delta z_o]^{1/2} w(z_l)\exp(j\omega_{ml}t) \quad , \tag{2}$$



SPIE Vol. 3571 • 0277-786X/99/$10.00

where $b=z_o/\Delta z_o+1$ if $z-z_o<c\tau/2$ and $b-1=l_1=c(t_{l_2}-\tau)/(2\Delta z_o)$ if $z-z_o\geq c\tau/2$; $l_2=c\,t_{l_2}/(2\Delta z_o)$; $z_l=l\Delta z_o$; $\Delta z_o=c\Delta t_o/2$ is the least spatial sampling interval and $\Delta t_o$ is the corresponding temporal sampling interval; $\omega_{ml}$ is $\omega_m(z)$ for $z$ between $(l-1)\Delta z_o$ and $l\Delta z_o$; $w=w_r+jw_i$ is a complex Gaussian random variable with zero mean value $\langle w(z)\rangle=\langle w_r(z)\rangle=\langle w_i(z)\rangle=0$, variance $Dw(z)=\langle|w(z)|^2\rangle=1$, and covariance $cov_w(z_k,z_l)=\langle w^*(z_k)w(z_l)\rangle=0$ for $k\neq l$.

## 3. ALGORITHMS FOR ESTIMATION OF DOPPLER VELOCITY

In this section we briefly describe the pulse-pair algorithm, a frequently used Doppler-velocity estimator, as well as the algorithms derived by us recently[2]. All this estimators (estimation algorithms) are based on the analysis of the heterodyne-signal autocovariance

$$Cov(t,\theta)=\langle I^*(t)I(t+\theta)\rangle \tag{3}$$

that depends in general not only on the temporal shift $\theta$ but on the moment $t$ as well.

### 3.1. PP Algorithm

This algorithm is based on the following estimate $\hat{\omega}_{mpp}(t_{l_2}=2z_{l_2}/c)$ of the range-dependent intermediate frequency $\omega_m(z)$ [see also Eq.(2)]:

$$\hat{\omega}_{mpp}(t_{l_2}=2z_{l_2}/c)=(\Delta t_o)^{-1}arctg\left[\mathrm{Im}Cov(t_{l_2},\Delta t_o)/\mathrm{Re}Cov(t_{l_2},\Delta t_o)\right], \tag{4}$$

where

$$Cov(t_{l_2},\Delta t_o)=M^{-1}\sum_{k=0}^{M}I^*(t_{l_2}+k\Delta t_o)I[t_{l_2}+(k+1)\Delta t_o]\ . \tag{5}$$

Because of the time averaging (instead of ensemble averaging) and finite pulse duration the least possible range resolution cell $\Delta_{res}$ is equal to

$$\Delta_{res}=c(M\Delta t_o+\tau)/2\ . \tag{6}$$

When $\Phi(z)$ and $V(z)$ do not change essentially over a $\Delta_{res}$ - long range interval, the PP algorithm provides the authentic profile $V(z)$ of the radial aerosol velocity. In the opposite case the profile obtained is as if a result of moving averaging with a $\Delta_{res}$ - wide window. Let us also mention that there is another covariance-based estimator, PPP estimator, that is a little more accurate, but more complicated modification of the PP algorithm.

### 3.2. Algorithms for improving the resolution of long-pulse coherent Doppler lidars

Taking into account the incoherent character of the aerosol scattering, on the basis of Eq.(1) we obtain the following analytical expression of the covariance $Cov(t,\theta)$:

$$Cov(t,\theta)=\int_{c(t+\theta-\tau)/2}^{ct/2}dz'\Phi(z')\exp[j\omega_m(z')\theta]\ . \tag{7}$$

From Eq.(7) one can derive the following algorithms for retrieving $\omega_m(z)$:

$$\omega_m(z=ct/2)=\left\{\Phi[c(t-\tau)/2]\omega_m[c(t-\tau)/2]+\mathrm{Im}[(2/c)Cov^{\mathrm{II}}_{t\theta}(t,\theta=0)]\right\}[\Phi(ct/2)]^{-1}\ , \tag{8a}$$

$$\omega_m(z=ct/2)=\theta^{-1}arctg\left\{\frac{(2/c)\,\mathrm{Im}Cov^{\mathrm{I}}_t(t,\theta)+\Phi[c(t+\theta-\tau)/2]\sin\{\omega_m[c(t+\theta-\tau)/2]\theta\}}{(2/c)\,\mathrm{Re}Cov^{\mathrm{I}}_t(t,\theta)+\Phi[c(t+\theta-\tau)/2]\cos\{\omega_m[c(t+\theta-\tau)/2]\theta\}}\right\}, \tag{8b}$$

where $\mathrm{Re}Cov(t,\theta)=\langle J(t)J(t+\theta)\rangle+\langle Q(t)Q(t+\theta)\rangle$, $\mathrm{Im}Cov(t,\theta)=\langle J(t)Q(t+\theta)\rangle-\langle J(t+\theta)Q(t)\rangle$, $\varphi^q(y)$ ($q$=I, II, III,...) denotes $q$th derivative of $\varphi$ with respect to $y$, and the quantities $[c(t-\tau)/2]$, $[c(t+\theta-\tau)/2]$, and $\{\omega_m[c(t+\theta-\tau)/2]\theta\}$ are arguments of $\Phi$, sin and cos respectively. Let us note that at distances $z<c\tau/2$ the algorithm (8b) is essentially simplified because then $\Phi(z)=0$. Besides, this algorithm is a generalization of the PP algorithm for the case of nonuniform distribution of $\Phi(z)$ and $V(z)$ within every $c\tau/2$ - long interval along the line of sight. On the basis of Eqs.(8a) and (8b), at sufficiently low noise level, one can determine $V(z)$ with a resolution step even of the order of the sampling interval. Herewith, the estimates of $Cov(t,\theta)$ should be obtained by a real ensemble averaging over a sufficient number of laser shots. The presence of derivatives in Eqs. (8a) and (8b) would multiply the speckle-noise effects and lead to the necessity of averaging over a large number of laser shots to effectively lower the noise level. So a considerable improvement of the spatial resolution is achievable at the expense of lowering the temporal resolution. The reducing of the speckle-noise

effects, and thus of the number of laser shots required, will improve the temporal resolution. For this purpose one should use suitable filtering or smoothing of the estimates $\hat{Cov}(t,\theta)$ and $\hat{V}(z)$ of $Cov(t,\theta)$ and V(z) respectively. In general, it is useful and interesting to compare by computer simulations the spatial and temporal resolution scales attainable by PP algorithm and algorithms (8a) and (8b).

## 4. SIMULATIONS

We have performed simulations with the use of various distributions, along the line of sight, of the radial velocity V($z$) and the signal power $\propto\Phi(z)$. Below we present results for a model of wind vortex which is convenient for testing the resolution of radial-velocity estimators because of its small spatial size and sharp velocity variations. The models of V($z$) and the maximum-resolved signal power profile $\Phi(z)$ are shown in Fig.1 and Fig.2, respectively. We assume that the profile $\Phi(z)$ has been determined with high accuracy by use of $Cov(t,0)$ and the deconvolution techniques[6]. The realizations of $J(z=ct/2)$ and $Q(z=ct/2)$ are generated on the basis of Eq.(2). Such a pair of realizations at $\lambda_o = 2\pi c/\omega_o = 10.6$ μm, $\omega_h = \omega_o$, and $\tau = 4$ μs is shown in Fig.3.

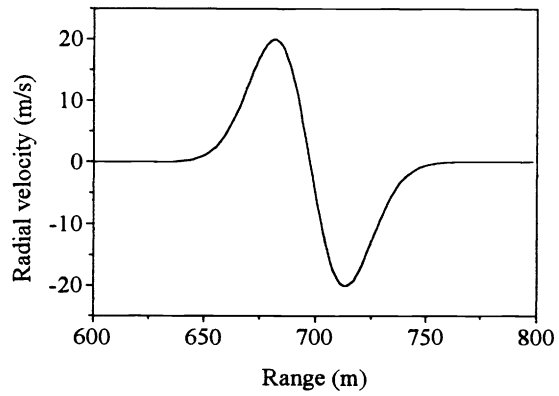


**Figure 1**. Model of the radial wind velocity as a function of range.

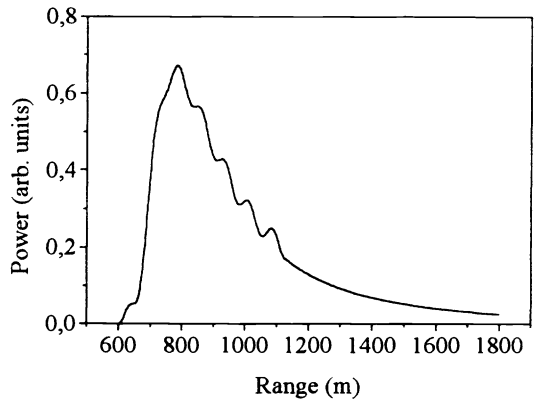


**Figure 2.** Model of the maximum-resolved signal power profile as a function of range.

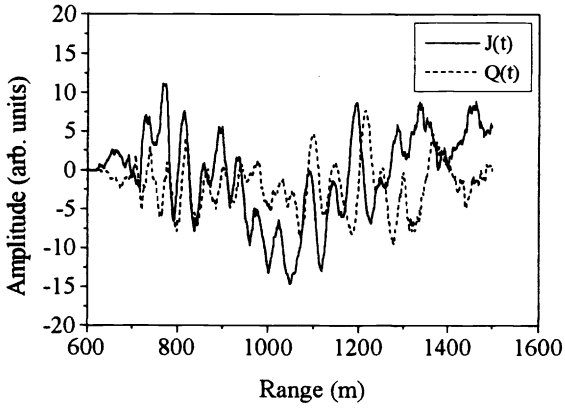


**Figure 3.** Example of a simulated signal for $\lambda_o = 2\pi c/\omega_o = 10.6$ μm and $\tau = 4$ μs . The inphase $J(t)$ (solid curve) and the quadrature $Q(t)$ (dashed curve) components of the signal are presented.

The estimates $\hat{Cov}(t,\theta)$ of the autocovariance function are obtained as an arithmetic mean:

$$\hat{Cov}(t = t_{l_2}, \theta = q\Delta t_o) = N^{-1}\sum_{k=1}^{N} I_k^*(t_{l_2}) I_k(t_{l_2} + q\Delta t_o) \ , \qquad (9)$$

where $N$ is the number of realizations employed. The covariance estimate (9) is destined for the long-pulse algorithms [Eqs.(8a),(8b)] to be applied to. The PP-algorithm performance is entirely based on Eqs.(4) and (5). The temporal sampling interval is $\Delta t_o = 10$ ns and corresponds to a spatial sampling step $\Delta z_o = 1.5$ m. We have not considered any additive-noise effects because they are much smaller than the speckle-noise effects.

The PP algorithm is first applied for processing the generated heterodyne signal. The number of sampling points having been used for PP estimation of V($z$) is $M$ = 20 [See Eq.(5)]. Two pulse durations are examined, $\tau$ = 200 ns for $\lambda_o$ = 2 μm and $\tau$ = 4 μs for $\lambda_o$ = 10.6 μm. Also, to reduce additionally the speckle-noise effect, the covariance estimate $Cov(t_{l_2}, \Delta t_o)$ [Eq.(5)] is averaged over a series of $N$ = 500 laser shots [$N$ generated realizations of $I(t)$]. The retrieved profiles $V_r(z)$ are shown in Fig.4, together with the original profile V(z). It is seen that at $\tau$ = 200 ns (Fig.4a) the noise is practically entirely removed, but there are considerable errors due to averaging along the line of sight. The retrieved extremal velocities are nearly twice lower (± 13 m/s instead of ± 20 m/s). The positive-to-negative peak positions are separated by approximately 42 m instead of 33 m. The overall resolution step achieved here is $\Delta_{res} = c(M\Delta t_o + \tau)/2$ = 60 m. In this case, the resolution can be improved (and the retrieving distortions avoided) by decreasing the sampling interval and pulse length, which would require extremely fast ADC and short-wavelength laser radiation. The negative effects due to the averaging are stronger in the case of longer laser pulses (Fig.4b, $\tau$ = 4 μs).

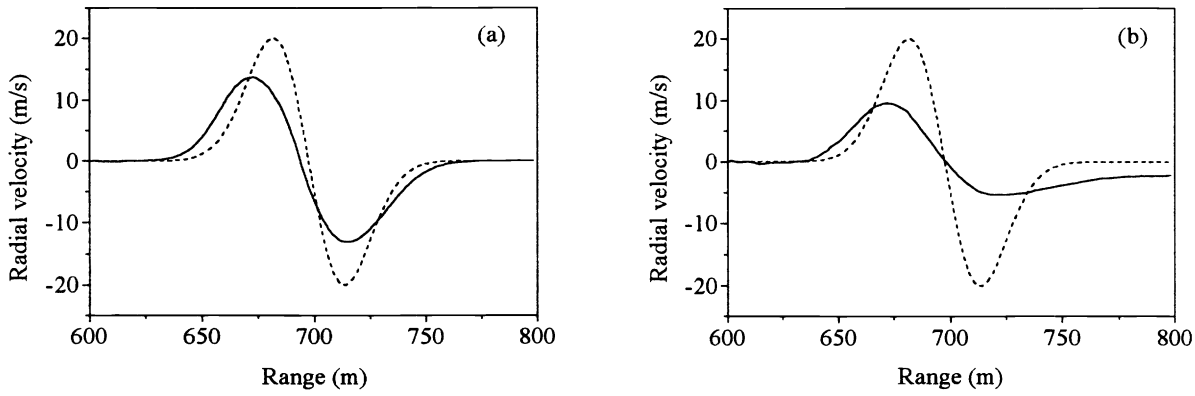


**Figure 4**. Profiles $V_r(z)$ restored by use of PP algorithm in the case of rectangular pulse with duration (a) $\tau$ = 200 ns ($\lambda_o$ = 2 μm) and (b) $\tau$ = 4 μs ($\lambda_o$ = 10.6 μm). The original profile V($z$) is given for comparison by the dashed curve.

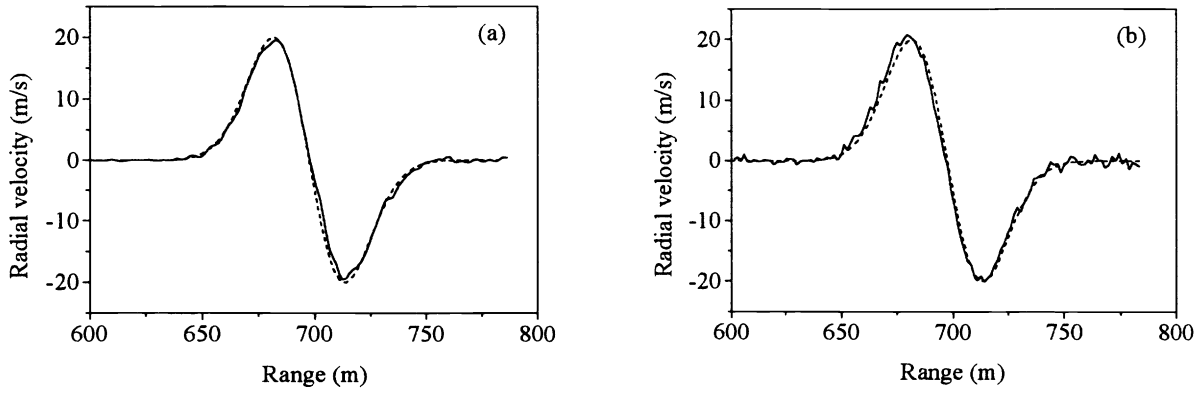


**Figure 5.** Profiles $V_r(z)$ restored by use of algorithm (8a) in the case of rectangular pulse with duration (a) $\tau$ = 200 ns ($\lambda_o$ = 2 μm) and (b) $\tau$ = 4 μs ($\lambda_o$ = 10.6 μm). The original profile V($z$) is given for comparison by the dashed curve.

Algorithms (8a) and (8b) are used for processing the same realizations of $I(t)$ as generated above. Generally, the longer the pulse duration the stronger the noise influence. Because of the recurrence character of the algorithm (8a), the noise error increases with the distance. Nevertheless, an acceptable restoration accuracy can be achieved by suitable filtration combined with ensemble averaging. Let us also note that the recurrence accumulation of the noise can be avoided by successive extending of the lidar dead zone [0,$z_o$] and investigating of not so long line-of-sight regions [$z_o$,$z$] whose length ($z$-$z_o$) is of the order of one or several pulse lengths. Due to the low spatial extent of the wind vortices the strong noise influence typical for this algorithm is damped. In Figs.5a and 5b we present the results for V($z$) restored by use of

algorithm (8a) for $\tau = 200$ ns ($\lambda_o = 2$ μm) and $\tau = 4$ μs ($\lambda_o = 10.6$ μm) respectively. They are obtained after filtering of $Cov(t,\theta)$ ($4\Delta t_o$ – wide window moving average and $\Delta t_o$ - long computing step) and averaging over $N = 10^4$ laser shots. The overall resolution cell achieved here is $\Delta_{res} \sim 4\Delta t_o = 6$ m.

Profiles V($z$) restored by use of algorithm (8b) are represented in Figs.6a and 6b, for $\tau = 200$ ns ($\lambda_o$=2 μm) and $\tau = 4$ μs ($\lambda_o = 10.6$ μm) respectively. The same filtration of $Cov(t,\theta)$ and the above-mentioned dead zone scanning approach are employed. The number of laser shots used is $N = 10^4$. The resolution cell achieved is again $\Delta_{res} = 6$ m. In general, both inverse algorithms permit one to reach considerably better spatial resolution than PP algorithm without decreasing the sampling interval, the pulse duration, and respectively the laser radiation wavelength. Certainly, a disadvantage to be overcome here is the necessity of powerful high pulse repetition rate lasers.

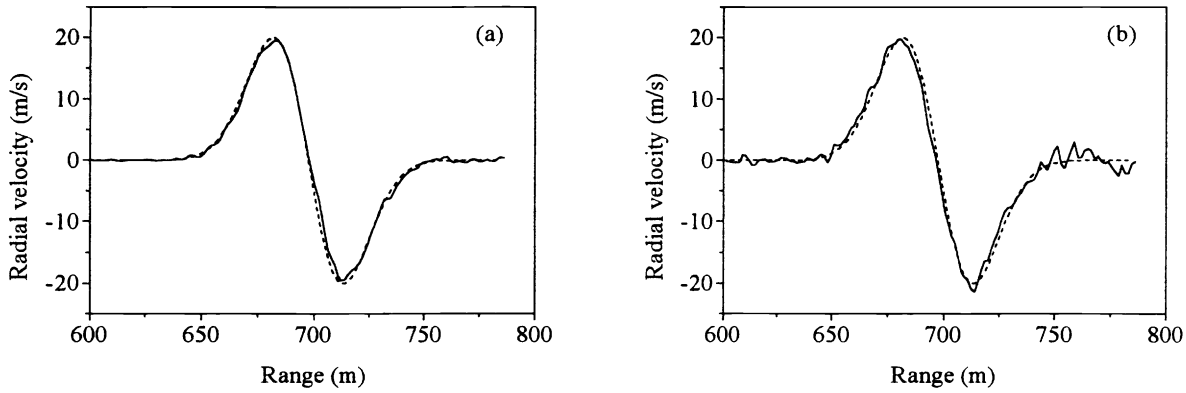


**Figure 6.** Profiles $V_r(z)$ restored by use of algorithm (8b) in the case of rectangular pulse with duration (a) $\tau = 200$ ns ($\lambda_o$=2 μm) and (b) $\tau = 4$ μs ($\lambda_o$=10.6 μm). The original profile V($z$) is given for comparison by the dashed curve.

## 5. CONCLUSION

The feasibilities are investigated by computer simulations of two new algorithms for high-resolution determination of Doppler-velocity profiles with coherent lidars. A comparison is done with the feasibilities of the well known PP algorithm. It is shown that the new algorithms allow one to achieve considerably better spatial resolution at longer sampling interval, pulse length and laser wavelength. At the same time the temporal resolution is lower because of the necessity of many laser shots to reduce the speckle-noise effect. Optimum filtering as well as a proposed here lidar dead-zone scanning technique lead to essential reducing of the noise and improving of the temporal resolution. A further searching for ways to improve the temporal resolution should evidently involve an optimization of the procedures of smoothing the signal covariance estimate and the retrieved Doppler-velocity profiles. The development of powerful, high pulse repetition rate lasers is also a factor of essential importance.

## 6. REFERENCES


1. P.R. Mahapatra and D.S. Zrnic', „Practical algorithms for mean velocity estimation in pulse Doppler weather radars using a small number of samples", *IEEE Trans. Geos. Remote Sens.*, **GE-21**, pp.491-501, 1983.
2. L.L. Gurdev, T.N. Dreischuh, and D.V. Stoyanov, „Algorithms for improving the resolution of long-rectangular-pulse coherent Doppler lidars", in preparation.
3. L.L. Gurdev, T.N. Dreischuh, and D.V. Stoyanov, „High-resolution processing of long-pulse-lidar data", *NASA Conference Publications* **3158** ( Part II), pp.637-640, 1992.
4. A. Dabas, Ph. Salamitou, D.Oh et al., „Lidar Signal Simulation and Processing", *Proc. 7th Conference on Coherent Laser Radar: Applications and Technology*, Paris, France, pp.221-228, 1993.
5. Ph. Salamitou, A. Dabas, and P. Flamant, „Simulation in the time domain for heterodyne coherent laser radar", *Appl. Opt.*, **34**, pp.499-506, 1995.
6. L.L. Gurdev, T.N. Dreischuh, and D.V. Stoyanov, „Deconvolution techniques for improving the resolution of long-pulse lidars", *J.Opt.Soc.Am.A*, **10**, pp.2296-2306, 1993.